

Chapter 14

Simulation and Optimization of Nanoparticle Patterned Substrates for SERS Effect

Mei Liu, Yan Peng and Zhizheng Wu

Abstract In order to make the best of the surface enhancing behaviors of metal nanostructures for Raman Scattering, a tactful balance should be found between signal enhancement, the distribution uniformity of ‘hot spots’ and the reproducibility of nanostructure patterned substrates, which should generally be testified by simulation and experiment. This paper simulated and compared the Raman enhancements produced from a variety of nanoparticle covered SERS substrates with different sizes and spaces, and it was concluded that the distance between the nanoparticles plays a contradictory role on the enhancement factor and the uniformity of the ‘hot spots’, and so it should be selected with comprehensive consideration.

Keywords Raman scattering • Surface enhancement Raman scattering (SERS) • Nanoparticles • Substrates

M. Liu (✉) · Y. Peng · Z. Wu

School of Mechatronics Engineering and Automation, Shanghai University,
Shanghai 200072, People’s Republic of China
e-mail: mliu@shu.edu.cn

Y. Peng

e-mail: pengyan@shu.edu.cn

Z. Wu

e-mail: zhizhengwu@shu.edu.cn

M. Liu

State Key Laboratory of Transducer Technology, Shanghai Institute of Microsystem
and Information Technology, Chinese Academy of Sciences, Shanghai 200050,
People’s Republic of China

14.1 Introduction

Surface-enhanced Raman scattering (SERS) is playing an increasing important role in biomedical research, biophysics and biochemistry, including single molecule detection, non-intrusive study of reaction dynamics, and also identification of tiny amounts of biological molecules or dangerous chemical species [1–3].

The fundamental physics of SERS has been extensively studied and generally understood [4]. Basically, the excitation of surface plasmons (SPs) in metal nanostructures can generate sizable electromagnetic field enhancements due to large transient surface dipoles induced by plasmons. Based on this principle, various types of substrates patterned with fine geometric nanostructures have been designed to increase the enhancement factor, and high SERS enhancements have been observed at certain spots of a substrate, making the detection of analytes possible at extremely low concentrations [5–9].

To provide more insight and understanding of the Raman scattering enhancement observed in previous publications, we have performed electromagnetic calculations by a finite element method using the commercial COMSOL multiphysics software package. For simplicity, the system was modeled as solid objects next to each other, which usually results in underestimating of actual field enhancements since local imperfections can enhance local fields drastically.

14.2 Establishment of the Models

In this paper, two types of simplified gold nanoparticles (NPs) models were constructed, simulated and compared to optimize substrates for SERS. The Gaussian electromagnetic wave follows the Maxwell equations in the simulated area, and boundary conditions at the interface between the scattering NPs and the medium. The scattering boundary condition, adsorption boundary condition and perfect matching layer condition was used in the simulation process. For SERS, it is generally agreed the Raman intensity increases by a factor $|E|^4$ and the Raman enhancement factor could be evaluated as [10]:

$$G(\mathbf{r}, \omega) = \left| \frac{E(\mathbf{r}, \omega)}{E_{\text{inc}}(\mathbf{r}, \omega)} \right|^4 \quad (14.1)$$

$$\text{Average}G(\omega) = \left| \frac{\text{Average}E(\omega)}{E_{\text{inc}}(\omega)} \right|^4 \quad (14.2)$$

where G and $\text{Average}G$ are two different factors to evaluate the maximum enhancement factor and the average enhancement factor in a fixed domain, $E(\mathbf{r}, \omega)$

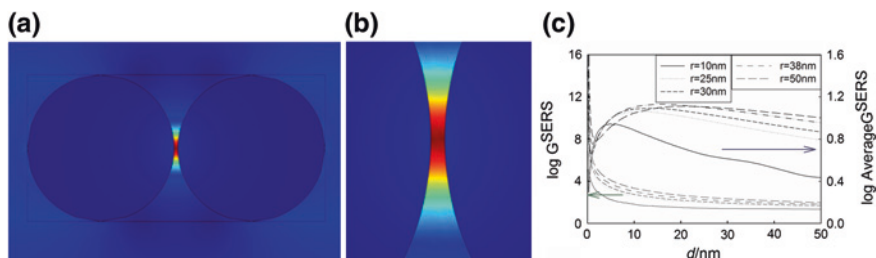


Fig. 14.1 The over-all electric field distribution between two NPs. **a** The electric field between two NPs. **b** The enlarged figure of the middle part of **a**. **c** The enhancement factor and average enhancement factor as a function of the distance d . *Arrows* in the figure indicates the respective axis each group of curve is corresponding to

is the overall electric field at location r , and $E_{inc}(r, \omega)$ is the electric field relating to the incident electric wave, $AverageE(\omega)$ is the average electric field strength in the fixed domain, and $E_{inc}(\omega)$ is the average electric field relating to the incident electric wave. The incident electromagnetic wave is polarized along the centerline of the NPs. The spot radius of the incident wave is equal to the laser wavelength, and the background electric field amplitude is 1 V/m.

14.2.1 Two Nanoparticles (NPs)

Here the electric field distribution between two NPs was simulated and obtained, shown in Fig. 14.1, where the radius r of the NPs is 10 nm, the distance d between the two NPs is 0.5 nm, and the wavelength λ of the electromagnetic wave is 785 nm.

The maximum enhancement factor and average enhancement factor between two NPs as a function of distance is shown in Fig. 14.1c, where λ is 785 nm. It can be seen that both enhancing factors decrease as the distances increases, with a big difference of 6 orders in enhancing factor as the distances changes from 0.7 to 10 nm. And the enhancing factors of smaller NPs tends to change more quickly, whose maximum AverageG reaches maximal at a smaller distance.

The calculated SERS enhancement at the hot spot is found to be able to reach 107–108, which may be sufficient for detection of a few molecules at the resonant frequency of the molecule. And from previous publications it is known that the nanostructure with curvature and dissymmetry is prone to increase the local field values. Considering that the experimental structures are more complicated and irregular than the models used in simulation, the realistic enhancement factor will be much higher and will be more beneficial for the detection of tiny amount of materials.

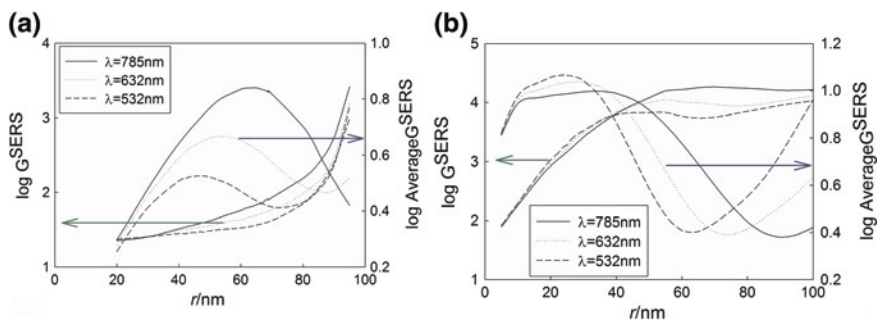


Fig. 14.2 **a** The enhancement factor and average enhancement factor as a function of the NP radius r when the pitch is fixed at 200 nm. **b** The enhancement factor and average enhancement factor as a function of the NPs radius r when the distance d is fixed at 5 nm

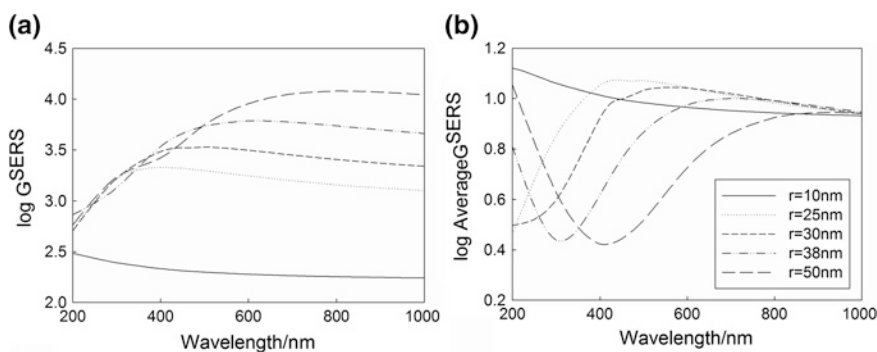


Fig. 14.3 The enhancement factor **(a)** and average enhancement factor **(b)** as a function of the incident wavelength λ when the distance between the NPs was set at 5 nm

With the pitch of the two NPs was fixed at 200 nm, the enhancement factors as a function of the sizes of NPs was shown in Fig. 14.2a. It can be seen that as the radius of the NPs increases, the enhancing factor increases monotonously, while the average enhancing factor has a peak, which shifts to a higher radius as the wavelength increases. When designing, a precise radius should be chosen to ensure both a high enhancing factor and a considerable average enhancing factor, and this is also true when the distance between the NPs is fixed, as shown in Fig. 14.2b.

With the distance between the NPs set at 5 nm, the enhancement factors as a function of the sizes of NPs was shown in Fig. 14.3. It can be seen that there is a peak for each case, indicating resonance between the NPs and the incident wave. And the location and strength of the peak both increases as the radius of the NPs increase, however, at the mean time, the average enhancement factors decrease—still there should be a balance between those parameters.

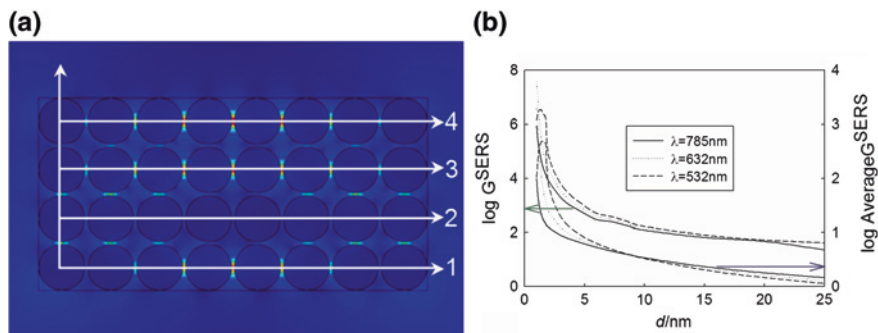


Fig. 14.4 **a** The over-all electric field distribution between arrays of NPs, where $d = 1$ nm, $r = 10$ nm, $\lambda = 532$ nm. The *white arrows* indicate the centerline of each array. **b** The enhancement factor and average enhancement factor of the NPs array as a function of the distance d

14.2.2 Array of Two NPs

Normally on SERS substrates, the nanostructures will most probably exist in the form of ordered arrays; so consequently, the distance between each nanostructures pairs is also one important issue that must be taken into account. Here ordered, not stochastic arrays were simulated.

Figure 14.4a shows the electric field distribution of the NPs array, with four white arrows indicating the centerline of each array. Apparently the electric distribution across the array is not uniform. Figure 14.4b shows the enhancement factor and average enhancement factor of the NPs array as a function of the distance d between the NPs. As the distance d increases, both enhancement factors will decrease, as expected.

Though the enhancing factors decreases as the distance increase, it could be clearly seen that as the distance increases from 1 to 10 nm for NPs of 10 nm radius, the uniformity of the enhancing factors gets better. The electric field strengths in the first column in Fig. 14.5 were quite discrete, with a big difference between each peak, meaning that electric field strength along the four centerlines deviate quite much from each other. The strength scattering can also be seen from Fig. 14.4a, where the distance between the NPs pairs were too close (1 nm), the electromagnetic wave along Line 2 is likely ‘blocked’ by the other NPs, with little enhancement between each NP on this line. The electric field strengths in the last two columns are smoother than the first one obviously.

So when designing a NP patterned SERS substrate, the NP array could not be too dense, which means, the distance between the NPs cannot be too small. However, if the NPs array were too loose, the enhancing effect will deteriorate and also the ‘hot spots’ would be too sparse, so a balance should be clarified for the NPs arrangement.

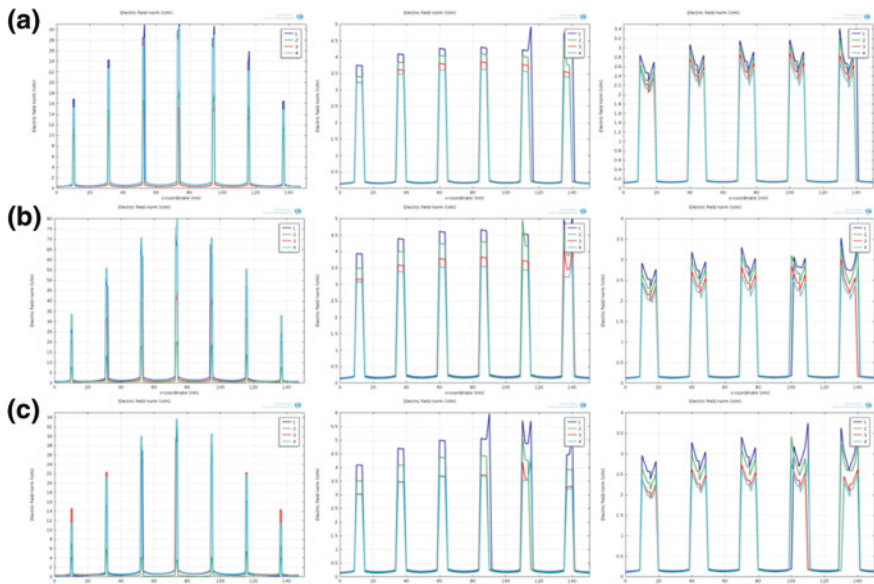


Fig. 14.5 The over-all electric field distribution along the *four centerlines* in Fig. 14.4a, where the radius of NPs is 10 nm. **a** $\lambda = 785$ nm, **b** $\lambda = 632$ nm, **c** $\lambda = 532$ nm. From *left to right*, the *three rows* of figure represent cases of $d=1$ nm, $d=5$ nm and $d=10$ nm, respectively

The geometrical parameters of the enhancement factor were demonstrated, and it can be concluded that the simulated results are in large scale in corresponding with published experimental results. And for a better uniform substrate, not only the size, distribution of the nanostructures should be optimized, but also the distance between the nanostructure pairs should be carefully defined.

14.3 Conclusions

To further reveal the physical mechanism of the enhancements of Raman scattering of gold NPs and to optimize the arrangement of NPs, we carried out thorough simulations of local field distributions. Two types of simplified gold NPs models, including smooth a NPs pair and a NP array, were calculated and compared. To both ensure a high maximal enhancement factor and a high average enhancement factor in a fixed domain, a new parameter AverageG was proposed. It can be concluded for a single pair of NPs, bigger NPs will result in a longer resonance wavelength. And as the distance gets longer, both the enhancement factor and the average enhancement factor will decrease dramatically. However, for a whole distribution of NPs on a whole substrate, if they are placed too close, the inner NPs

will be largely 'shielded'. So when it comes to a whole substrate, the distance between the NPs should be defined by carefully balancing the enhancement factors and their consistence.

Acknowledgments The work was supported by the National Natural Science Foundation of China (No. 51205245), Science and Technology Commission of Shanghai Municipality (No. 11PJ1403500), and Innovation Program of Shanghai Municipal Education Commission (No. 12YZ022).

References

1. Lim D-K et al (2009) Nanogap-engineerable Raman-active nanodumbbells for single-molecule detection. *Nat Mater* 9(1):60–67
2. Pieczonka NP, Aroca RF (2008) Single molecule analysis by surface-enhanced Raman scattering. *Chem Soc Rev* 37(5):946–954
3. Tripp RA, Dluhy RA, Zhao Y (2008) Novel nanostructures for SERS biosensing. *Nano Today* 3(3):31–37
4. Mishchenko MI, Travis LD, Lacis AA (2002) Scattering, absorption, and emission of light by small particles. Cambridge university press, Cambridge
5. Panigrahi S et al (2006) Self-assembly of silver nanoparticles: synthesis, stabilization, optical properties, and application in surface-enhanced Raman scattering. *J Phys Chem B* 110(27):13436–13444
6. Braun G et al (2007) Surface-enhanced Raman spectroscopy for DNA detection by nanoparticle assembly onto smooth metal films. *J Am Chem Soc* 129(20):6378–6379
7. Tao A et al (2003) Langmuir-Blodgett silver nanowire monolayers for molecular sensing using surface-enhanced Raman spectroscopy. *Nano Lett* 3(9):1229–1233
8. Li W-D et al (2011) Three-dimensional cavity nanoantenna coupled plasmonic nanodots for ultrahigh and uniform surface-enhanced Raman scattering over large area. *Opt Express* 19(5):3925–3936
9. Tian C et al (2011) Nanoparticle attachment on silver corrugated-wire nanoantenna for large increases of surface-enhanced Raman scattering. *ACS Nano* 5(12):9442–9449
10. Kneipp K et al (1997) Single molecule detection using surface-enhanced Raman scattering (SERS). *Phys Rev Lett* 78(9):1667–1670